THE JOURNAL OF PHYSICAL CHEMISTRY B

ARTICLE

pubs.acs.org/JPCB

Dielectric Relaxation Study of the Ion Solvation and Association of $NaCF_3SO_3$, $Mg(CF_3SO_3)_2$, and $Ba(ClO_4)_2$ in *N*,*N*-Dimethylformamide

Anna Płaczek,[†,‡] Glenn Hefter,[*,†] Hafiz M. A. Rahman,[‡] and Richard Buchner[*,‡]

[†]Chemistry Department, Murdoch University, Murdoch, WA 6150, Australia

[‡]Institut für Physikalische und Theoretische Chemie, Universität Regensburg, D-93040, Regensburg, Germany

Supporting Information

ABSTRACT: Solutions of sodium trifluoromethanesulfonate, magnesium trifluoromethanesulfonate, and barium perchlorate in *N*,*N*-dimethylformamide (DMF) have been investigated using broadband dielectric relaxation spectroscopy at 25 °C. All spectra were dominated by a solvent relaxation process centered at ~15 GHz but also exhibited one (for $NaCF_3SO_3$) or two (for the 2:1 salts) low-amplitude processes, centered at frequencies below 2 GHz, that could be attributed to the presence of ion pairs. Effective solvation numbers calculated from the solvent relaxation amplitudes indicated strong solvation of all three cations, with evidence for the formation of a second solvation sheath for Mg^{2+} and possibly Ba^{2+}. Detailed analysis of the solute-related processes showed that solvent-shared ion pairs (SIPs) were formed in $NaCF_3SO_3$ solutions in DMF. The data for $Mg(CF_3SO_3)_2$ and $Ba(ClO_4)_2$ solutions were not definitive but, consistent with the solvation evidence, favored the presence of double solvent-separated ion pairs and SIPs. Overall association constants, K_A, were small for all three salts in DMF and increased in the order: $NaCF_3SO_3 < Ba(ClO_4)_2 < Mg(CF_3SO_3)_2$.

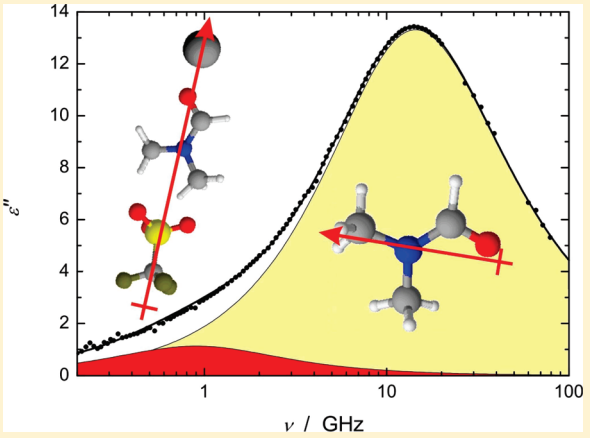

1. INTRODUCTION

Dielectric relaxation spectroscopy (DRS) is a widely applicable but relatively under-utilized technique for the study of electrolyte solutions.[1−3] In principle, it can provide detailed and quantitative information about both the dynamics and thermodynamics of such solutions and, in favorable cases, even structural insights. While most published DRS studies have been of aqueous systems, the technique is readily applicable to nonaqueous solutions. Molecular-solvent solutions investigated to date have included: propylene carbonate,[4,5] acetonitrile,[6,7] methanol,[8] formamide,[9,10] *N*-methylformamide,[9,10] and *N*,*N*-dimethylacetamide,[11] although such studies have in general been limited to a narrow range of monovalent (1:1) electrolytes.

Liquid *N*,*N*-dimethylformamide (DMF) is a versatile solvent for organic and inorganic substances and has been employed extensively as a solvent for polymers and paints and as a reaction medium.[12] It has a reasonably high dielectric constant (ε = 36.71 at 25 °C)[13] and a sizable dipole moment (μ = 3.86 D).[13] With a Gutmann donor number of 26.6,[13] DMF is a strong electron-density donor and thus a powerful solvator of cations. On the other hand, it is a rather poor solvator of anions, with a Gutmann acceptor number of just 16.0 (similar to acetonitrile and propylene carbonate).[13]

As might be expected from these generally favorable characteristics, the physicochemical properties of electrolyte solutions in DMF have been widely investigated. Such studies have included determinations of Gibbs energies,[14] enthalpies and entropies,[15] and viscosities,[16] although again most were restricted to relatively small numbers of 1:1 electrolytes. Recently, a comprehensive report of the molar volumes and heat capacities of a wide range of electrolytes, including non-1:1 charge types, has appeared.[17]

An ongoing problem for such studies is the reliable extrapolation to infinite dilution of experimental data measured at finite electrolyte concentrations to obtain the desired standard state properties. Because the extrapolation functions used for this purpose (such as the Redlich−Meyer and Pitzer equations)[18] assume that electrolytes are fully dissociated, this can lead to significant errors in the standard state values.[19] This difficulty is usually more pertinent to electrolyte solutions in nonaqueous solvents (because such solutions typically exhibit higher levels of ion association than their aqueous counterparts)[20,21] and becomes acute when dealing with salts containing higher-charged ions. While theoretical treatments have been developed that make allowance for ion association,[22] the required equilibrium constants are almost invariably lacking for nonaqueous solutions, and the available methods for estimating such quantities[21] are too

Received: December 7, 2010
Revised: January 11, 2011
Published: February 22, 2011

   dx.doi.org/10.1021/jp1116307 | *J. Phys. Chem. B* 2011, 115, 2234–2242

crude to be reliable. To minimize such errors most researchers have employed electrolytes containing weakly complexing counterions, such as perchlorate (ClO_4^-) for cations or tetraalkylammonium (R_4N^+) ions for anions, and then *assumed* complete dissociation. While this approach has produced many useful and self-consistent results it clearly has limitations. The justification for such a choice requires a better understanding of the competing processes of ion solvation and ion association of electrolytes in nonaqueous solvents.[3]

As already noted, DRS can provide useful insights into both ion solvation and ion association processes.[3] Solvation information can be obtained in a straightforward manner from DR spectra, which have produced a coherent picture of the solvation characteristics of a range of (mostly monovalent) ions in a variety of solvents.[6,7,9−11] The study of ion association by DRS is especially fruitful as this technique is very sensitive to the formation of weak complexes and has a unique ability to detect and quantify solvent-separated and contact ion pairs in solution.[1] Unlike many popular techniques for determining ion-association constants, DRS is equally applicable to aqueous and nonaqueous solutions and to symmetrical and nonsymmetrical electrolytes.[1,21]

The present study employs broadband DRS to investigate solutions of sodium trifluoromethanesulfonate (sodium "triflate", $NaCF_3SO_3$), magnesium triflate ($Mg(CF_3SO_3)_2$), and barium perchlorate ($Ba(ClO_4)_2$) in DMF at 25 °C. These salts were chosen to represent the range of electrolytes used in comprehensive thermodynamic investigations.[17] All three salts are readily soluble in DMF and, because of the low charge density of their anions, they are expected to be relatively weakly associated; i.e., they are nominally strong electrolytes in DMF. Except for a preliminary study[9] on $NaClO_4$, to the best of our knowledge the only previous DRS investigation of electrolyte solutions in DMF is that of Wurm et al.[11] who reported spectra for lithium, sodium, and tetra-*n*-butylammonium perchlorates at 25 °C over a frequency range similar to that employed here. The present paper is the first to provide information on nonsymmetrical electrolytes.

2. EXPERIMENTAL SECTION

2.1. Reagents. Sodium and magnesium triflates were prepared by neutralization of suspensions of Na_2CO_3 and MgO, respectively, in methanol (analytical reagent grade) with trifluoromethanesulfonic ("triflic") acid (3M, AR grade), as described elsewhere.[17] The products were recrystallized from AR ethanol and dried under vacuum at 50 °C for several days. Hydrated barium perchlorate was prepared by neutralization of an aqueous suspension of BaO with perchloric acid (UNIVAR, AR grade, 72% w/w). The $Ba(ClO_4)_2$ hydrate so obtained was recrystallized twice from water and then dehydrated and dried under vacuum at 150 °C for 4 days. Solvent *N*,*N*-dimethylformamide (Merck, AR grade, 99.5%) was dried and stored over freshly activated 3 Å molecular sieves and had a typical water content of <200 ppm (coulometric Karl Fischer titration). Solvent for solution preparation was taken from an undisturbed storage vessel by syringe immediately prior to use. Solutions were prepared by weight in a drybox, without buoyancy corrections.

2.2. Instrumentation and Measurements. Dielectric measurements at frequencies $0.2 \lesssim \nu/\mathrm{GHz} \leq 20$ were performed at Murdoch University using a Hewlett-Packard model HP 85070 M Dielectric Probe System, consisting of an HP 8720D vector network analyzer (VNA) and an HP 85070 dielectric probe kit. Additional coaxial-line reflection measurements were carried out in Regensburg with an Agilent E8364B VNA combined with Agilent 85070E-020 (0.2−20 GHz) and 85070E-050 (0.5−50 GHz) probes. Both VNAs were calibrated using air, mercury, and *N*,*N*-dimethylacetamide (Fluka, > 99.8%, stored over activated 4 Å molecular sieves) as standards. Each solution was measured at least twice using independent calibrations, with relative permittivity, $\varepsilon'(\nu)$, and total loss, $\eta''(\nu)$, recorded at 101 frequencies equidistant on a logarithmic scale. Most solutions were also measured at higher frequencies ($27 \leq \nu/\mathrm{GHz} \leq 89$) at Regensburg University using two waveguide interferometers. Detailed descriptions of these instruments and the measurement principles have been published previously.[23,24] All DRS measurements (VNAs and interferometers) were made at 25 ± 0.02 °C, with a NIST-traceable accuracy of ±0.05 °C. The probable maximum errors in ε' and η'' are 2% of the static permittivity of the sample.

Solution densities, ρ, were determined at 25 ± 0.01 °C at Regensburg using a vibrating-tube densimeter (Paar DMA 60/601HT) calibrated with nitrogen (ρ = 1.1456 mg·cm^{-3})[25] and water (ρ = 0.997043 g·cm^{-3}).[25] Electrical conductivities, κ, were measured at 25 ± 0.005 °C, over the frequency range $0.1 \leq \nu/\mathrm{kHz} \leq 10$ with an accuracy of ±0.5%, using an AC bridge and capillary cells as described elsewhere.[26−28] Infinite-frequency resistances, $R_\infty = \lim_{\nu\to\infty} R(\nu)$, were obtained by extrapolation using the empirical function $R(\nu) = R_\infty + A/\nu^a$, where A is specific to the cell and $a \approx 0.5$.[28,29]

2.3. Calculations. DRS involves measurement of the complex relative dielectric permittivity $\hat{\varepsilon}(\nu)$ of a sample as a function of the frequency ν of an applied electromagnetic field

$$\hat{\varepsilon}(\nu) = \varepsilon'(\nu) - i\varepsilon''(\nu) \quad (1)$$

where $\varepsilon'(\nu)$ is the relative permittivity and $\varepsilon''(\nu)$ is the dielectric loss.[30,31] The latter is obtained from the measurable total loss

$$\eta''(\nu) = \varepsilon''(\nu) + \kappa/(2\pi\nu\varepsilon_o) \quad (2)$$

where ε_o is the permittivity of free space. A typical spectrum for $\eta''(\nu)$ and the corresponding $\varepsilon''(\nu)$ is shown in Figure S1 of the Supporting Information. The conductivity contribution ($\kappa/2\pi\nu\varepsilon_o$) ultimately swamps the signal of interest ($\varepsilon''(\nu)$) at low frequencies and thus determines the minimum frequency for meaningful DR measurements.[32] In principle, κ is accessible from separate (low-frequency conductivity) measurements, but in practice, for reasons discussed at length elsewhere,[32] it is usually treated as an adjustable parameter in the data-fitting procedure. Nevertheless, experimental κ values were taken as the starting approximation in the fitting process at each concentration, and the fit and experimental results always agreed to better than 5%.

Conductivity-corrected experimental spectra were fitted with plausible models based on n individual relaxation processes

$$\hat{\varepsilon}(\nu) = \sum_{j=1}^{n} \frac{S_j}{(1 + (i2\pi\nu\tau_j)^{1-\alpha_j})^{\beta_j}} + \varepsilon_\infty \quad (3)$$

with each dispersion step j of amplitude S_j and relaxation time τ_j being modeled using either a Havriliak−Negami (HN) equation, with relaxation-time distribution parameters $0 \leq \alpha_j < 1$ and $0 < \beta_j \leq 1$, or any of its simplified variants: the Debye (D; $\alpha_j = 0, \beta_j = 1$), Cole−Cole (CC; $\beta_j = 1$), or Cole−Davidson (CD; $\alpha_j = 0$) models. The static (relative) permittivity of the sample is defined as $\varepsilon = \Sigma S_j + \varepsilon_\infty$ where $\varepsilon_\infty = \lim_{\nu\to\infty} \varepsilon'(\nu)$ is the so-called infinite-frequency permittivity. The preferred model was that which gave the lowest value of the reduced error function (χ^2)[33] *and*

relaxation amplitudes and times that were physically realistic and varied smoothly with solute concentration. Additionally, selected spectra were analyzed with a recently published procedure[34] that allows an unbiased determination of the number of relaxation processes required for the formal description of $\hat{\varepsilon}(\nu)$. Typical results from these analyses are given in the Supporting Information, Figures S4−S6.

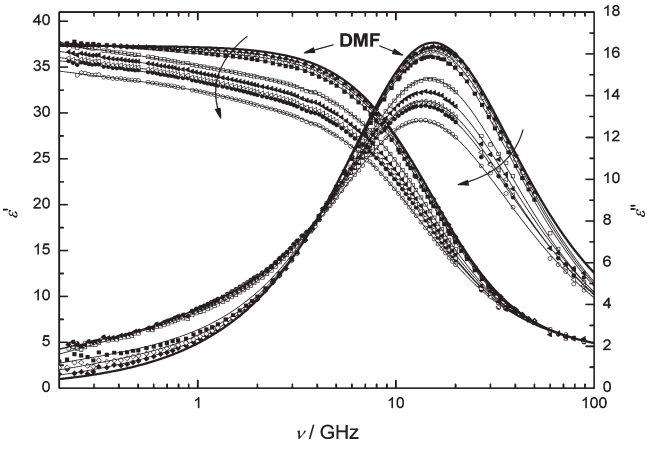

Figure 1. Permittivity, $\varepsilon'(\nu)$, and dielectric loss, $\varepsilon''(\nu)$, spectra of neat DMF and solutions containing various concentrations of $Ba(ClO_4)_2$ in DMF at 25 °C. The curved arrows indicate increasing solute concentration (as listed in Table 1). Lines are fits using the D + D + CD model; heavy lines denote the neat solvent spectra.

3. RESULTS AND DISCUSSION

3.1. Process Assignment. A typical set of experimental spectra (for $Ba(ClO_4)_2$) obtained for the present electrolyte solutions in DMF is shown in Figure 1. Equivalent data for $NaCF_3SO_3$ and $Mg(CF_3SO_3)_2$ solutions are given in the Supporting Information (Figures S2 and S3). Values of the parameters obtained by application of eq 3 to the experimental spectra are summarized in Table 1, which also includes densities, experimental conductivities, and χ^2 values. A full discussion of the various quantities in Table 1 is given below.

The DR spectra of all of the present electrolyte solutions in DMF are dominated by a large-amplitude process centered at ca. 15 GHz (Figure 1 and Supporting Information Figures S2 and S3). This process is readily assigned, by comparison with the spectrum for neat DMF[35] (Figure 1), to the rotational diffusion of solvent molecules. A detailed study[35] of the temperature

Table 1. Densities, Conductivities, and Fitting Parameters (Using D + CD or D + D + CD Models) of the DR Spectra for DMF Solutions of $NaCF_3SO_3$, $Mg(CF_3SO_3)_2$, and $Ba(ClO_4)_2$ at 25 °C[a]

c	ρ	κ	ε	S_{IP1}	τ_{IP1}	S_{IP2}	τ_{IP2}	S_S	τ_S	β	ε_∞	$10^3\,\chi^2$
						$NaCF_3SO_3$						
0.0	0.943838[b]	0.0	37.31						10.4		3.02	
0.0478			37.19	0.48	360			32.74	10.6	0.970	3.98	18.3
0.1024			37.23	1.10	374			32.20	10.9	0.957	3.92	8.7
0.1832	0.962874	0.761	35.89	1.81	228			29.54	10.7	0.999	4.54	11.9
0.2858	0.973380	1.063	34.72	2.14	180		n/a	28.17	11.0	0.981	4.42	15.5
0.3303	0.977963	1.251	34.25	2.25	175			28.03	11.5	0.941	3.97	10.5
0.3647	0.981400	1.334	33.89	2.27	177			28.13	12.2	0.885	3.50	7.6
0.4183	0.986753	1.454	33.08	2.41	165			27.39	12.8	0.850	3.29	13.0
						$Mg(CF_3SO_3)_2$						
0.0137			37.82	0.71	640	0.16	200[c]	33.16	10.6	0.965	3.79	8.4
0.0280			37.89	0.87	542	0.37	199	32.73	10.7	0.963	3.92	5.5
0.0466			37.87	1.09	450	0.51	168	32.29	10.9	0.960	3.98	11.5
0.1100	0.967286	0.823	37.40	1.26	419	2.13	159	30.46	11.6	0.908	3.55	4.2
0.1607	0.977882	1.080	36.40	1.35	363	2.35	129	29.12	12.0	0.895	3.58	3.9
0.1858	0.983110	1.189	35.84	1.41	314	2.30	120	28.61	12.3	0.880	3.52	4.5
0.1940	0.984790	1.221	35.68	1.45	313	2.35	114	27.95	12.0	0.913	3.93	13.9
0.2359	0.993617	1.376	34.88	1.49	288	2.35	106	27.46	12.9	0.863	3.57	9.6
0.2866	1.004146	1.523	34.20	1.46	363	2.79	99	26.17	13.2	0.866	3.78	11.4
						$Ba(ClO_4)_2$						
0.0141			37.49	0.56	330	0.00	-	33.00	10.5	0.974	3.93	4.6
0.0273			37.79	0.85	471	0.34	194	32.58	10.6	0.976	4.02	6.7
0.0465			38.19	1.21	630	0.81	183	32.10	10.8	0.971	4.07	13.2
0.1000	0.971526	0.870	38.00	1.90	492	2.21	141	29.85	11.1	0.952	4.03	8.0
0.1463	0.984269	1.169	37.68	1.97	714	2.85	139	29.24	12.0	0.897	3.62	6.1
0.1771	0.992814	1.334	37.02	1.99	723	3.01	128	28.37	12.2	0.888	3.64	5.2
0.1929	0.997180	1.416	36.78	2.01	788	3.09	129	28.29	12.7	0.859	3.39	5.7
0.2460	1.011665	1.649	35.63	2.03	773	3.17	119	27.03	13.3	0.835	3.39	4.6

[a] Units: c in mol L^{-1}; ρ in g cm^{-3}; κ in S m^{-1}; τ_j in ps; ε, ε_∞, S_j, and β are dimensionless. [b] Neat DMF densities varied slightly between runs and were 0.943 910 for $Mg(CF_3SO_3)_2$ and 0.943 816 for $Ba(ClO_4)_2$ solutions. [c] Fixed value.

dx.doi.org/10.1021/jp1116307 |J. Phys. Chem. B 2011, 115, 2234–2242

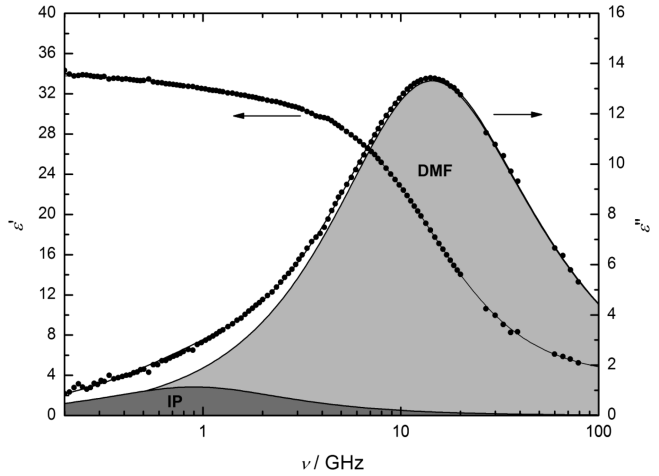

Figure 2. Permittivity, $\varepsilon'(\nu)$, and dielectric loss, $\varepsilon''(\nu)$, spectra of 0.3647 mol L^{-1} $NaCF_3SO_3$ in DMF at 25 °C. The shaded areas show the contributions of the ion-pair (IP) and of the solvent relaxation process (DMF) to $\varepsilon''(\nu)$.

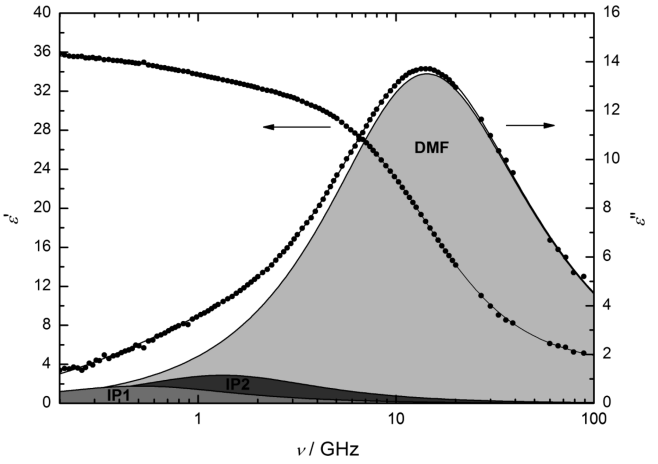

Figure 3. Permittivity, $\varepsilon'(\nu)$, and dielectric loss, $\varepsilon''(\nu)$, spectra of 0.1858 mol L^{-1} $Mg(CF_3SO_3)_2$ in DMF at 25 °C. The shaded areas show the contributions of two ion-pairs (IP1 and IP2) and of the solvent relaxation process (DMF) to $\varepsilon''(\nu)$.

dependence of the DR spectrum of neat DMF revealed additional small but systematic effects at high frequencies, probably arising from low-energy librational modes and molecular inertia. For fitting purposes, these effects were formally described with a small-amplitude Debye process centered at ca. 150 GHz.[35] However, in the present study these small deviations were accounted for by fitting the DMF spectrum with an asymmetrically broadened (Cole−Davidson) model. This approach has the advantage of requiring one less fitting parameter than a two-D model,[35] which aids the overall fitting of the DR spectra of the salt solutions.

In addition to the dominant solvent relaxation, the present DR spectra for all three sets of salt solutions in DMF showed either one ($NaCF_3SO_3$) or two ($Mg(CF_3SO_3)_2$ and $Ba(ClO_4)_2$) low-frequency Debye processes centered at $\nu < 2$ GHz. The presence of these low-frequency modes was essential for an accurate fit of the observed spectra at low frequencies and was confirmed by the recently developed method for bias-free determination of the number of relaxation processes required for the formal fit of a given spectrum[34] (Supporting Information, Figures S4−S6). From their location in the spectrum and the concentration dependence of their amplitudes, all of these low-frequency processes can be assigned with confidence to the rotational diffusion of ion pairs in solution. The triflate anion also has a dipole moment that must therefore contribute to the observed spectra. However, because it is fairly small and has a relatively low dipole moment ($\mu_- \approx 3.6$ D from quantum mechanical calculations),[36] the contribution from the triflate ion is small over the investigated concentration ranges and probably occurs at relatively high frequencies. It is therefore reasonable to assume that the triflate mode is subsumed by the much more intense solvent relaxation without significantly affecting the quantitative interpretation of the latter.

Overall fits of the spectra were achieved, therefore, with either a two-process (D + CD; for $NaCF_3SO_3$) or a three-process (D + D + CD; for $Mg(CF_3SO_3)_2$ and $Ba(ClO_4)_2$) model. The quality of the fits obtained and the contributions of the individual processes to the observed spectra are summarized in Table 1 and illustrated for $NaCF_3SO_3$ and $Mg(CF_3SO_3)_2$ in Figures 2 and 3, respectively. Fits for $Ba(ClO_4)_2$ in DMF were similar to the latter (Supporting Information, Figure S7). A quantitative analysis of the spectra is given below.

3.2. Solvent Relaxation and Ion Solvation. A representative plot, for $Mg(CF_3SO_3)_2$, of the dispersion amplitude (relaxation strength, S_s) of the major solvent process at 15 GHz, observed in all of the present solutions in DMF, is included (uppermost curve) in Figure 4(a). The corresponding relaxation times, τ_s, are plotted (lowermost curve) in Figure 4(b). Similar data were obtained for the other two sets of salt solutions (Supporting Information, Figures S8 and S9). For all of the present salt solutions, the magnitude of S_s decreases steadily with solute concentration, c, which is indicative of strong ion solvation.

The extent of ion−solvent interactions can be quantified using the generalized Cavell equation[37]

$$c_j = \frac{3(\varepsilon + (1-\varepsilon)A_j)}{\varepsilon} \cdot \frac{k_B T \varepsilon_o}{N_A} \cdot \frac{(1-\alpha_j f_j)^2}{g_j \mu_j^2} \cdot S_j \qquad (4)$$

normalized with respect to the pure solvent. In eq 4, S_j is the amplitude, c_j the concentration, μ_j the dipole moment, α_j the polarizability of the relaxing species, ε (= $\lim_{\nu\to 0}\varepsilon'(\nu)$) the static permittivity of the solution, and T the thermodynamic temperature in Kelvin, and k_B and N_A are, respectively, the Boltzmann and Avogadro constants. The reaction-field and cavity-field factors, f_j and A_j, are defined by the size and shape of the rotating dipole,[30] while the static (Kirkwood) dipole−dipole correlation factor, g_j, accounts for orientational correlation of neighboring species of the same kind. For the present reasonably dilute solutions it was assumed that the correlation factor of the solvent is independent of the salt concentration and thus cancels out in the normalization of eq 4. This is reasonable as the value of g_j is close to unity in neat DMF,[35] consistent with the absence of significant long-range dipole−dipole correlations of the solvent molecules.

Effective solvation numbers for the solute were obtained from the solvent dispersion amplitudes as described previously.[24,38] Briefly, this involves correction of the observed solvent dispersion amplitude for kinetic depolarization (kd), which is related to the movement of the solvated ions in the applied field. The kd was calculated using the Hubbard−Onsager continuum model.[39,40] The apparent concentration of rotationally free solvent molecules,

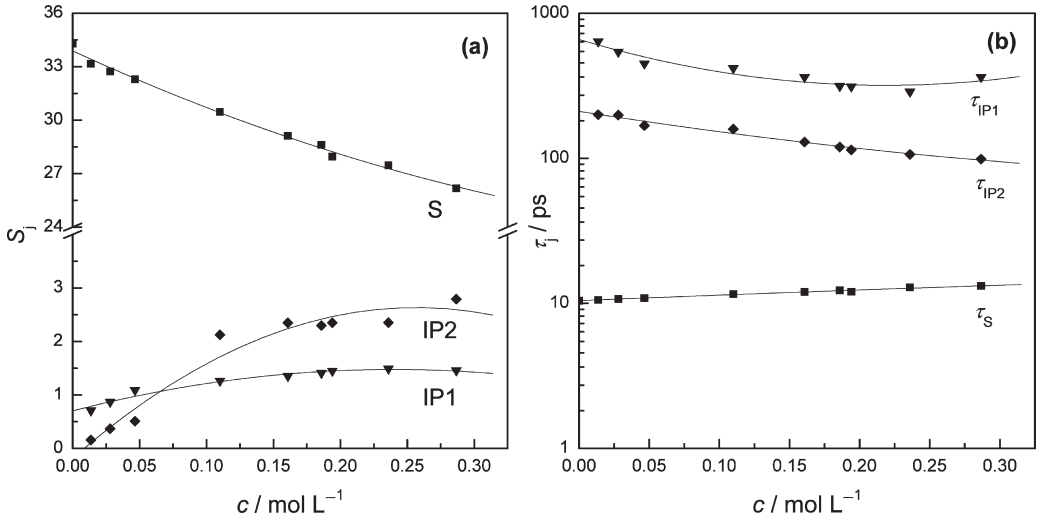

Figure 4. (a) Dispersion amplitudes, S_j, and (b) relaxation times, τ_j, as functions of solute concentration for DMF solutions of $Mg(CF_3SO_3)_2$ at 25 °C (lines included only as a visual guide).

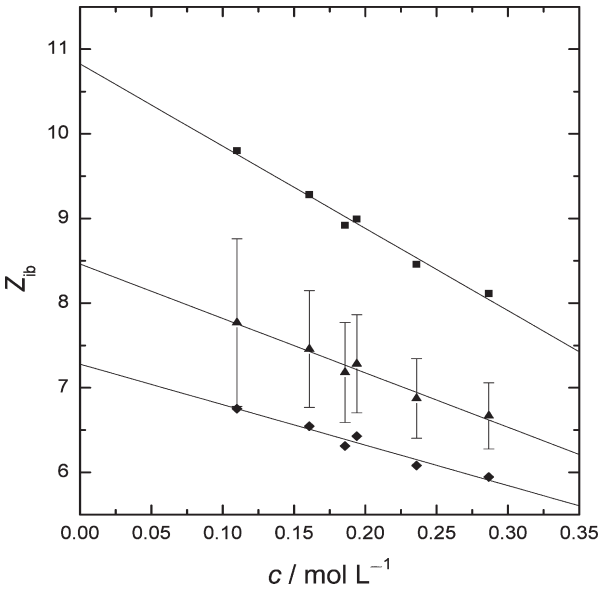

Figure 5. Effective solvation numbers, Z_{ib}, for $Mg(CF_3SO_3)_2$ in DMF at 25 °C as a function of solute concentration under various transport boundary conditions: ■ no kd, ▲ slip kd, ♦ stick kd. Error bars correspond to the standard deviation of a fit of the equation $S_S(c) = S_S(0)$ [=34.29] $+ a_1c + a_2c^{3/2}$ to the experimental solvent amplitudes.

c_s^{ap}, was then determined for three limiting cases: negligible kd and kd with ion transport under *slip* or *stick* boundary conditions. Subtraction of c_s^{ap} from the analytical (total) solvent concentration, c_s, then allows determination of the effective solvation number, Z_{ib}, the number of irrotationally bound (ib) solvent molecules per "particle" of solute

$$Z_{ib} = (c_s - c_s^{ap})/c \qquad (5)$$

where c is the (total) electrolyte concentration in the solution. As defined, Z_{ib} can be thought of as the average number of solvent molecules per solute particle "frozen" on the DR time scale and thus not contributing to the solvent relaxation process.[38]

Typical results obtained for $Z_{ib}(c)$ in $Mg(CF_3SO_3)_2$ solutions in DMF are shown in Figure 5. Similar values were determined for the other two sets of salt solutions (Supporting Information, Figures S10 and S11). Note that the increase in the uncertainty in $Z_{ib}(c)$ as $c \rightarrow 0$ is normal. This is because, while the uncertainty of S_s (estimated as one standard deviation of the fit of the empirical equation $S_s(c) = S_s(0)$ [=34.29] $+ a_1c + a_2c^{3/2}$ to the experimental solvent amplitudes) and thus of c_s^{ap} is constant, the uncertainty in $Z_{ib}(c)$ rises as both $(c_s - c_s^{ap})$ and $c \rightarrow 0$. Within these uncertainty limits, Z_{ib} was found to vary smoothly with c for all three systems and ion-transport boundary conditions. The infinite dilution values, $Z_{ib}(0)$, obtained by linear extrapolation of $Z_{ib}(c)$ are collected in Table 2. As would be expected, they vary in the order *stick* < *slip* < no kd for each electrolyte; *slip* conditions are generally considered to be the most realistic for the dielectric relaxation of solvated ions.[3]

Table 2. Effective Solvation Numbers at Infinite Dilution, $Z_{ib}(0)$, for $NaCF_3SO_3$, $Mg(CF_3SO_3)_2$, and $Ba(ClO_4)_2$ in DMF Solutions at 25 °C Obtained with Various Ion-Transport Boundary Conditions[a]

electrolyte	$Z_{ib}(0)$ (no kd)	$Z_{ib}(0)$ (*slip*)	$Z_{ib}(0)$ (*stick*)
$NaCF_3SO_3$	6.2(3)	5.0(3)	4.4(3)
$Mg(CF_3SO_3)_2$	10.8(2)	8.5(2)	7.3(2)
$Ba(ClO_4)_2$	13.4(6)	10.6(6)	9.3(6)

[a] Numbers in parentheses are standard deviations in the last digit, derived from linear least-squares fits.

Literature data show that neither $CF_3SO_3^-$ nor ClO_4^- is well solvated in DMF,[11,41−44] consistent with the low charge density of both ions and the poor acceptor properties of DMF.[13,20] This suggests that it is reasonable to assume that $Z_{ib}(CF_3SO_3^-) \approx Z_{ib}(ClO_4^-) \approx 0$ in DMF and thus, following Wurm et al.,[11] that the Z_{ib} values given in Table 2 can be assigned fully to the cations. The present results therefore indicate that at infinite dilution in DMF the cation Na^+ has an effective solvation number on the DRS time scale of ~5, which is essentially the same as the value of $Z_{ib}(0) = 4.9 \pm 0.3$ derived for Na^+ by Wurm et al. from DRS measurements on $NaClO_4$ in DMF assuming *slip* conditions.[11] The Z_{ib} values for both Mg^{2+} and Ba^{2+} (Table 2) suggest at least partial formation of a second solvation sheath. This is undoubtedly true for Mg^{2+}, which is certainly too small ($r_+ = 72$ pm)[45] to

accommodate the likely number of immobilized solvent molecules (~9) in its first coordination shell.

The present $Z_{ib}(0)$ values for the cations in DMF (Table 2) can be compared with those obtained from DRS measurements in water, ~4.5 and ~14 for Na^+ and Mg^{2+}, respectively, under *slip* boundary conditions (Ba^{2+} does not appear to have been studied by DRS in aqueous solution).[3] The similarity of Z_{ib}-(Na^+) in DMF and H_2O is a little surprising at first glance, given the much greater molecular size of DMF, but the present results are broadly compatible with the solvation numbers reported for Na^+ in DMF of ~3 (from transference measurements)[46] and ~6 (from NMR data).[47] Also, it has to be kept in mind that Z_{ib} is mainly determined by the strength of ion−solvent interactions, whereas coordination numbers are more sensitive to packing requirements. For Mg^{2+} the present value of $Z_{ib} \approx 9$ in DMF is considerably smaller than that observed in H_2O, which is a reflection of the highly developed second hydration shell of Mg^{2+}(aq) associated, at least in part, with extensive H-bonding. On the other hand the present value in DMF is rather larger than the (solid state) coordination number of six DMF molecules obtained from single-crystal X-ray diffraction studies[48,49] and the (solution) solvation number, also ~6, estimated by Raman spectroscopy in DMF solutions.[50] These differences reflect the greater role of packing effects in determining coordination numbers, as well as the sensitivity of Raman to nearest-neighbor interactions. The present value of $Z_{ib}(Ba^{2+})_{DMF} \approx 10.6$ (Table 2) is slightly larger than the value of 8.4 obtained from Raman data[50] and again implies at least the partial existence of a second solvation shell.

3.3. Solute Relaxations and Ion Association. Ion association in electrolyte solutions is usually best described by the well-known Eigen−Tamm model[51]

$$M^{n+} + L^- \overset{K_1}{\leftrightarrow} \underset{2SIP}{[MS_2L]^{(n-1)+}} \overset{K_2}{\leftrightarrow} \underset{SIP}{[MSL]^{(n-1)+}} \overset{K_3}{\leftrightarrow} \underset{CIP}{[ML]^{(n-1)+}} \quad (6)$$

in which solvated ions initially combine with their solvation sheaths essentially intact, to form double solvent separated ion pairs (2SIPs). The 2SIPs may then lose their intervening oriented solvent molecules (S) to form successively solvent-shared (SIPs) and contact (CIPs) ion pairs. While the Eigen−Tamm mechanism (eq 6) is thought to be generally applicable, this does not mean that all species will be present (or at least detectable) in any given electrolyte/solvent mixture.

The DMF solutions of all three investigated electrolytes exhibit a low-amplitude but well-defined solute-related relaxation process centered at $\nu < 1.0$ GHz (Figures 2 and 3 and Supporting Information Figure S7). In addition, both $Mg(CF_3SO_3)_2$ and $Ba(ClO_4)_2$ show an additional process centered at ~2 GHz. From their location in the spectra and the concentration dependence of their amplitudes, these low-frequency processes can be attributed to the presence of ion pairs in solution. To help to establish which ion-pair types are present, it is useful to compare the observed ion-pair relaxation times with calculated values.

Ion-Pair Relaxation Times. The observable macroscopic relaxation time τ_{obs} for a Debye process is a collective property that can be related to the corresponding molecular rotational correlation time τ'_{obs} via the Powles−Glarum equation[52,53]

$$\tau_{obs} = \frac{3\varepsilon}{2\varepsilon + \varepsilon_\infty} \cdot \tau'_{obs} \quad (7)$$

Table 3. Comparison of Experimental, τ'_{obs},[a] and Calculated Rotational Correlation Times for *Stick* and *Slip* Boundary Conditions, τ'_{stick} and τ'_{slip},[b] for Ion-Pair Reorientation in Salt Solutions in DMF at 25 °C[c]

electrolyte	τ'_{obs}	IP	τ'_{slip}	τ'_{stick}
$NaCF_3SO_3$	122	CIP	7	105
		SIP	102	310
		2SIP	348	697
$Mg(CF_3SO_3)_2$	104 (τ_2)	CIP	4	94
	299 (τ_1)	SIP	88	284
		2SIP	318	653
$Ba(ClO_4)_2$	103 (τ_2)	CIP	8	65
	478 (τ_1)	SIP	96	228
		2SIP	323	551

[a] Obtained via the Powles−Glarum relation (eq 7). [b] Obtained from the SED relation (eq 8). [c] Unit: τ_j in ps.

The τ'_{obs} values can be compared with the theoretical values of the rotational correlation time, τ', calculated from the molecular volume of rotation, V_r, and the bulk solution viscosity, η, via the Stokes−Einstein−Debye equation[54,55]

$$\tau' = \frac{3V_r}{k_B} \cdot \frac{\eta}{T} \quad (8)$$

Solution viscosities were assumed, in the absence of experimental data, to be the same as neat DMF (0.802 mPa s).[13] The value of V_r is obtained via the relationship $V_r = V_m f_\perp C$, where V_m is the (geometric) molecular volume of the rotating species; $f_\perp$ is a shape factor; and C is the hydrodynamic coupling constant between the rotating species and its environment ($C = 1$ for *stick* or $C = 1 - f_\perp^{-2/3}$ for *slip* boundary conditions). For convenience, the ion pairs were approximated as prolate ellipsoids when calculating $f_\perp$ using the approach of Dote and Kivelson.[54]

Microscopic relaxation times obtained using eq 8 for all plausible ion-pair types rotating under *slip* and *stick* hydrodynamic boundary conditions are collected in Table 3 along with the observed molecular rotational correlation times. Unfortunately, comparisons of the observed results (calculated via eq 7) with those calculated using the SED model (eq 8) do not unequivocally identify the relaxing species in the present solutions. Considering the simplest system ($NaCF_3SO_3$) first, the τ'_{obs} value of 122 ps is consistent with either a SIP rotating under *slip* conditions or a CIP under *stick* conditions (Table 3). As *slip* conditions are generally considered more likely for dissolved molecular-level species,[55] this implies (but does not prove) the presence of SIPs rather than CIPs, which is also consistent with the strong solvation of Na^+ by DMF and the weak solvation of $CF_3SO_3^-$ (Section 3.2).

For solutions of $Mg(CF_3SO_3)_2$ and $Ba(ClO_4)_2$ in DMF, the situation is also not clear-cut. The observed relaxation times for the two solute-related processes centered at $\nu < 2$ GHz appear to be consistent with either a combination of SIPs and 2SIPs rotating under *slip* boundary conditions or a CIP + SIP combination rotating under *stick* conditions (Table 3). The former would appear to be more likely, consistent with the preference of *slip* conditions for molecular rotation[55] and the evidence from the Z_{ib} values for the existence of at least a partial second solvation shell around the doubly charged cations (Section 3.2). Nevertheless, it must be recognized that, while the SED equation (originally derived for

macroscopic bodies rotating in a continuous medium) works surprisingly well for molecular-level entities,[54,55] significant approximations must be made in calculating the relaxation times.[54] For example, a more sophisticated analysis of the solvated ion-pair geometry, e.g., by making allowance for the specific orientation of the intervening solvent molecule(s),[8] might be necessary to produce more realistic values of IP rotational correlation times.

Ion-Pair Concentrations. The observed solute-related amplitudes (collectively labeled S_{IP}) can be used to estimate the corresponding ion-pair concentrations (c_{IP}) via the Cavell equation. As the types of ion pairs present are not known a priori, the required input parameters for eq 4, α_j, g_j, f_j, A_j, and μ_j, were calculated for all plausible ion-pair structures. Polarizabilities of the ion pairs were estimated assuming: $\alpha_{IP} = \alpha_+ + \alpha_- + n\alpha_{DMF}$, with $\alpha/4\pi\varepsilon_o$Å^3 = 0.211 (Na^+),[56] 0.111 (Mg^{2+}),[57] 1.50 (Ba^{2+}),[58] 6.84 ($CF_3SO_3^-$),[59] 5.45 (ClO_4^-),[58] 7.88 (DMF),[35] and n = 0, 1, or 2. Because the ion-pair concentrations are low, interactions between them should be negligible, and so g_{IP} values were assumed to be unity throughout. The field factors f_j and A_j were calculated by standard procedures.[37] Evaluation of the ion-pair dipole moments μ_j, which represent the major uncertainty in calculating ion-pair concentrations via eq 4, is discussed in the following section.

Estimation of Ion-Pair Dipole Moments. The dipole moment of an ion pair in solution, μ_{IP}, is given by

$$\mu_{IP} = \mu^o_{IP} - \mu_{ind} - n\mu_s - \mu_- \qquad (9)$$

which involves adjustment of μ^o_{IP}, the gas-phase dipole moment, for the presence of n (= 0, 1, or 2) oriented solvent molecules of dipole moment μ_s between the ions, for the induced dipole moment, μ_{ind}, due to the polarizabilities of the ions,[60] and for the dipole moments of the ions themselves.[37] For the salts studied here, only the triflate ion has a dipole moment (μ_- = 3.60 D).[36]

The values of μ^o_{IP} for the monovalent electrolyte $NaCF_3SO_3$ ($z_+ = |z_-| = 1$) were calculated as[37]

$$\mu^o_{IP} = ze_o d \qquad (10)$$

where e_o is the elementary charge and d the distance between the charges ($d = r_+ + r_- + 2nr_s$, where n = 0, 1, or 2 for CIPs, SIPs, and 2SIPs, respectively). Calculation of μ^o_{IP} for the charged ion pairs, $MgCF_3SO_3^+$ and $BaClO_4^+$, formed in solutions of the two asymmetric electrolytes, is less straightforward because the reference point is no longer uniquely defined. A natural choice of reference point is the pivot of the charged dipole.[37] For a spherocone with $C_{n\infty}$ symmetry, the pivot is located on the symmetry axis at a point o_B defined by the positions of the cation and anion centers (o_+ and o_-), yielding[37]

$$\mu^o_{IP} = e_o|z_+(o_+ - o_B) + z_-(o_- - o_B)| \qquad (11)$$

The center of hydrodynamic stress was taken as the pivot, o_B, as it is more appropriate for dipole rotation in a viscous medium than the center of mass.[37] The radii assumed for the calculation of the ion-pair dipole moments were:[45] r_+/pm = 102 (Na^+), 72 (Mg^{2+}), 136 (Ba^{2+}); r_-/pm = 307 ($CF_3SO_3^-$, taken as an ellipsoid)[61] and 240 (ClO_4^-), and r_s/pm = r_{DMF} = 330.[35] Induced dipole moments were calculated as

$$\mu_{ind} = \frac{d^4(z_-\alpha_+ + z_+\alpha_-) + 2(z_+ + z_-)d\alpha_+\alpha_-}{d^6 - 4\alpha_+\alpha_-} \cdot e_o \qquad (12)$$

The μ_{IP} values obtained from these calculations are summarized in Table 4. Dipole moments for the CIPs[62] were also calculated with MOPAC[36] to crosscheck the above approach, although such calculations for ion pairs are not without their problems.[63] For $NaCF_3SO_3^0$ (μ_{IP} = 13.0 D) and $BaClO_4^+$ (16.0 D), the MOPAC-calculated moments agree very well with the corresponding values listed in Table 4 (14.0 and 17.4 D, respectively). For $MgCF_3SO_3^+$, the difference (21.7 vs 27.1 D) is larger, which can be attributed in part to the different reference points of the two calculations (MOPAC uses the center of mass). Nevertheless, the comparison lends credence to the calculation procedure (eqs 9−12) which at present is the only route to μ_{IP} values for SIPs and 2SIPs.

Table 4. Estimated Ion-Pair Dipole Moments, μ_{IP}, and Standard Overall Association Constants, K^o_A, for DMF Solutions of $NaCF_3SO_3$, $Mg(CF_3SO_3)_2$, and $Ba(ClO_4)_2$ at 25 °C[a]

	$NaCF_3SO_3$		$Mg(CF_3SO_3)_2$			$Ba(ClO_4)_2$		
	μ_{IP}	K^o_A	μ_{IP}	K^o_A		μ_{IP}	K^o_A	
CIP	14.0	68 ± 16	27.1			17.4		
SIP	43.6	**5 ± 2**	51.3	**84 ± 7**[b]	224 ± 11[c]	38.2	**21 ± 6**[b]	48 ± 1500[c,d]
2SIP	71.7	2.2 ± 0.7	71.9			55.3		

[a] Units: μ_{IP} in D; K^o_A in L mol^{-1}. Preferred K^o_A values (see text) in bold underline. [b] Combined 2SIP + SIP model. [c] Combined SIP + CIP model. [d] The large uncertainty is an artifact of the fitting process.

Ion-Pair Formation. Assuming only species of 1:1 stoichiometry are formed, the overall ion association constant for an electrolyte, K_A, can be expressed as

$$K_A = \frac{c_{IP}}{c_+c_-} \qquad (13)$$

where here c_{IP} is the *total* ion pair concentration (i.e., the sum of all IP types present) and c_+ and c_- are the *free* ion concentrations. Combination of c_{IP} determined from eq 4 and the usual mass balance relationships gives K_A at each value of the electrolyte concentration, c. The standard state (infinite dilution) constant K^o_A can then be obtained from $K_A(c)$ using, for example, a Guggenheim-type equation[11]

$$\log K_A = \log K^o_A - \frac{2A_{DH}|z_+z_-|\sqrt{I}}{1 + a_K\sqrt{I}} + b_K I + c_K I^{3/2} \qquad (14)$$

where A_{DH} (= 1.5554 L$^{1/2}$ mol$^{-1/2}$)[64] is the Debye−Hückel constant for DMF; y_K ($y = a, b, c$) are empirical parameters; and I is the stoichiometric ionic strength ($I = (1/2)\sum_i c_i z_i^2$).[11]

The overall association constants, $K_A(c)$, for $NaCF_3SO_3$ in DMF obtained via eqs 4 and 13 assuming only SIPs were formed are plotted against I in Figure 6. Extrapolation to infinite dilution with eq 14 gave a standard value of $K^o_A = (5 \pm 2)$ L mol^{-1}, which is comparable with the value of 4.2 L mol^{-1} reported for SIPs for $NaClO_4$ in DMF, also obtained by DRS.[11] As expected, quite different values of K^o_A are obtained if different types of ion pairs are assumed to be present (Table 4). However, as noted above, the DRS data for $NaCF_3SO_3$ appear to be most consistent with the presence of SIPs alone, which suggests that the degree of association of this salt in DMF is very small. This finding vindicates the assumption of complete dissociation for this salt in previous thermodynamic studies.[17] It would be useful to compare the present K^o_A value with, e.g., conductivity measurements; however, to the best of our knowledge, no such data are available in the literature, and it should be noted that the quantification of such a weak association using conventional techniques such as conductometry is not a trivial task.[21]

Interpretation of the ion association data for both $Mg(CF_3SO_3)_2$ and $Ba(ClO_4)_2$ is complicated by the presence in the DR spectra of

the two strongly overlapping but weak ion-pair modes. This produces parameter coupling in the fit, which in turn affects the accuracy with which the ion-pair amplitudes can be determined (Figure 4 and Supporting Information, Figure S9). Even so, bias-free fitting[34] clearly shows there are two low-frequency modes in the DR spectra of both 2:1 salts (Supporting Information, Figures S5 and S6). As usual, the overall level of ion association is strongly dependent on the nature of the IPs taken to be present (Table 4). Consistent with the Z_{ib} values and the assumption of *slip* boundary conditions (see above), assignment of the two low-frequency processes (Figures 3 and S6) to the rotational diffusion of 2SIPs (centered at $\nu \approx 0.2$ GHz) and SIPs (centered at $\nu \approx 1.5$ GHz) seems most plausible. The K_i values obtained on the basis of this model are plotted in Figure 7 for both $Mg(CF_3SO_3)_2$ and $Ba(ClO_4)_2$ solutions in DMF. As would be expected from the reaction scheme summarized in eq 6, the values of $K_2(c)$, which correspond to an equilibrium that involves only a change in solvation, are virtually independent of I (the decreases in $K_2(c)$ at $I \lesssim 0.3$ mol L^{-1} are almost certainly a reflection of errors), while K_1 and therefore K_A ($= K_1 + K_1K_2$), which involve charged species, show the expected increase as $I \rightarrow 0$.

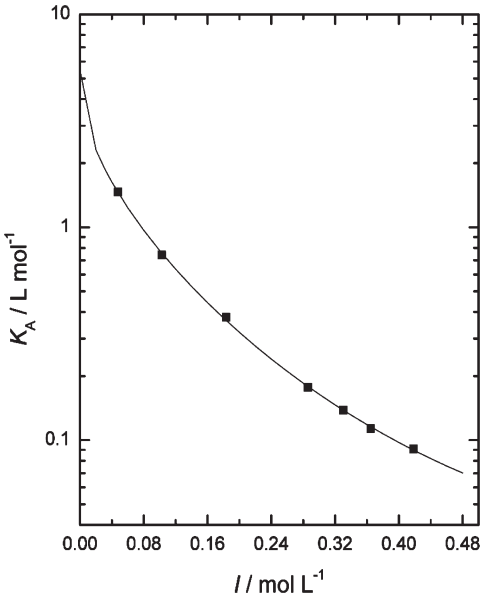

Figure 6. Overall association constant, K_A, for $NaCF_3SO_3$ in DMF at 25 °C as a function of ionic strength, I, assuming only SIPs are present. The curve represents the fit obtained using eq 14 with the y_K values listed in the Supporting Information (Table S1).

On the basis of the 2SIP + SIP model, it appears that both $Mg(CF_3SO_3)_2$ and $Ba(ClO_4)_2$ are only moderately associated in DMF at 25 °C, with K_A° values of just 84 and 21 L mol^{-1}, respectively (Table 4). As for $NaCF_3SO_3$, there are no data available in the literature that are directly comparable with the present values. Nevertheless, a K_A° of 182 L mol^{-1} has been reported[7] for $Mg(ClO_4)_2$ in acetonitrile using a combination of DR and infrared spectroscopies. While acetonitrile has a dielectric constant and acceptor number that are similar to those of DMF, it is a much weaker cation solvator (electron-density donor),[20] which implies a higher level of ion association than in DMF. The results for both of the present 2:1 electrolytes suggest that ion association will have only relatively minor effects on the determination of their thermodynamic properties in DMF,[17] especially when it is remembered that the association constants of higher-charged electrolytes decrease quickly with increasing concentration (Figure 7).

4. CONCLUDING REMARKS

The present DR spectra have shown that all three cations, Na^+, Mg^{2+}, and Ba^{2+}, are strongly solvated in DMF with indications of a well-developed second solvation shell for Mg^{2+} and to a lesser extent for Ba^{2+}. Detailed analysis of the spectra have indicated the presence of only SIPs in DMF solutions of $NaCF_3SO_3$ and two types of ion pairs (most likely SIPs and 2SIPs) in $Mg(CF_3SO_3)_2$ and $Ba(ClO_4)_2$ solutions. The overall level of association for all three salts was low, with standard association constants (K_A°) increasing in the order: $NaCF_3SO_3$ < $Ba(ClO_4)_2$ < $Mg(CF_3SO_3)_2$. These results support, to some extent, the widespread assumption of complete dissociation of these and related electrolytes in thermodynamic studies.

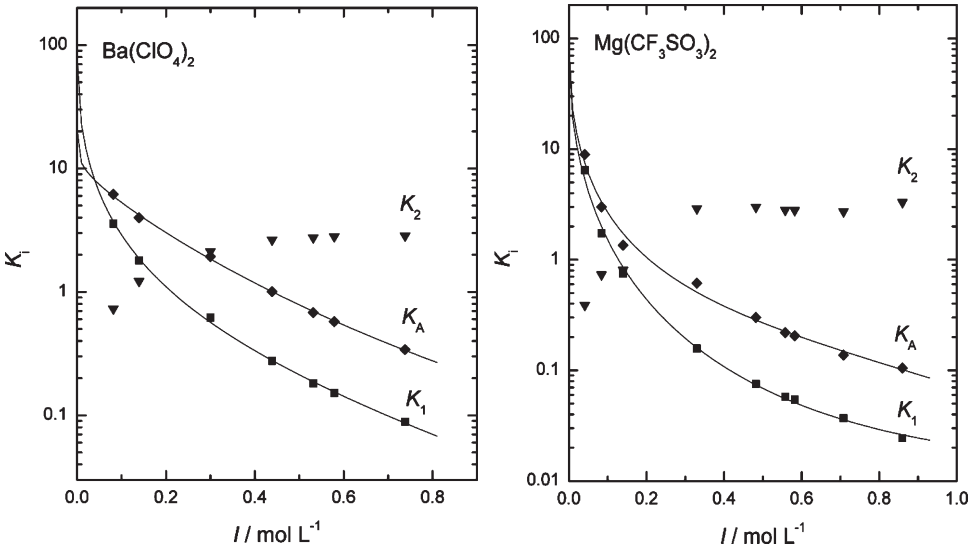

Figure 7. Overall association constants, K_A, and stepwise formation constants K_1 and K_2 as functions of ionic strength, I, assuming a 2SIP + SIP model for DMF solutions of $Ba(ClO_4)_2$ and $Mg(CF_3SO_3)_2$ at 25 °C. Curves for K_A and K_1 were obtained using eq 14 with the y_K values for K_A listed in the Supporting Information, Table S1.

dx.doi.org/10.1021/jp1116307 |J. Phys. Chem. B 2011, 115, 2234–2242

■ ASSOCIATED CONTENT

Supporting Information. Figures showing the conductivity contribution, the relaxation-time distribution functions obtained with the method of ref 34, and figures analogous to Figures 1, 3, 4, and 5 for the other electrolytes. This material is available free of charge via the Internet at http://pubs.acs.org.

■ AUTHOR INFORMATION

Corresponding Author

*E-mail: g.hefter@murdoch.edu.au; richard.buchner@chemie.uni-regensburg.de.

■ ACKNOWLEDGMENT

Murdoch University and the German Academic Exchange Service (DAAD) are gratefully acknowledged for funding AP's stays in Australia and Germany, respectively. HMAR thanks the Higher Education Commission of Pakistan for financial support. AP thanks Prof. Wacław Grzybkowski for his ongoing encouragement.

■ REFERENCES

(1) Buchner, R. Dielectric Spectroscopy of Solutions. In *Novel Approaches to the Structure and Dynamics of Liquids: Experiments, Theories and Simulations*; Samios, J., Durov, V. A., Eds.; Kluwer: Dordrecht, Netherlands, 2004.
(2) Buchner, R. *Pure Appl. Chem.* **2008**, *80*, 1239.
(3) Buchner, R.; Hefter, G. *Phys. Chem. Chem. Phys.* **2009**, *11*, 8984.
(4) Barthel, J.; Feuerlein, F. *J. Solution Chem.* **1984**, *13*, 393.
(5) Barthel, J.; Feuerlein, F. *Z. Phys. Chem.* **1986**, *148*, 157.
(6) Barthel, J.; Kleebauer, M.; Buchner, R. *J. Solution Chem.* **1995**, *24*, 1.
(7) Eberspächer, P.; Wismeth, E.; Buchner, R.; Barthel, J. *J. Mol. Liq.* **2006**, *129*, 3.
(8) Buchner, R.; Hefter, G. *J. Solution Chem.* **2002**, *31*, 521.
(9) Barthel, J.; Bachhuber, K.; Buchner, R. *Z. Naturforsch., A: Phys. Sci.* **1995**, *50*, 65.
(10) Wurm, B.; Baar, C.; Buchner, R.; Barthel, J. *J. Mol. Liq.* **2006**, *127*, 14.
(11) Wurm, B.; Münsterer, M.; Richardi, J.; Buchner, R.; Barthel, J. *J. Mol. Liq.* **2005**, *119*, 97.
(12) Chadwick, S. S. *Encyclopedia of Industrial Chemistry*; Wiley-VCH: Weinheim, 2006.
(13) Marcus, Y. *The Properties of Solvents*; John Wiley: London, 1998.
(14) Kalidas, C.; Hefter, G.; Marcus, Y. *Chem. Rev.* **2000**, *100*, 819.
(15) Hefter, G.; Marcus, Y.; Waghorne, W. E. *Chem. Rev.* **2002**, *102*, 2773.
(16) Jenkins, H. D. B.; Marcus, Y. *Chem. Rev.* **1995**, *95*, 2695.
(17) Płaczek, A.; Grzybkowski, W.; Hefter, G. *J. Phys. Chem. B* **2008**, *112*, 12366.
(18) Pitzer, K. S. *Activity Coefficients in Electrolyte Solutions*, 2nd ed.; CRC Press: Boca Raton, USA, 1991.
(19) Marcus, Y.; Hefter, G. *Chem. Rev.* **2004**, *104*, 3405.
(20) Marcus, Y. *Ion Solvation*; Wiley: New York, 1985.
(21) Marcus, Y.; Hefter, G. *Chem. Rev.* **2006**, *106*, 4585.
(22) Côté, J.-F.; Desnoyers, J. *J. Solution Chem.* **1999**, *28*, 396.
(23) Barthel, J.; Bachhuber, K.; Buchner, R.; Hetzenauer, H.; Kleebauer, M. *Ber. Bunsen-Ges. Phys. Chem.* **1991**, *95*, 853.
(24) Barthel, J.; Buchner, R.; Eberspächer, P.-N.; Münsterer, M.; Stauber, J.; Wurm, B. *J. Mol. Liq.* **1998**, *78*, 83.
(25) Lide, D. R. *CRC Handbook of Chemistry and Physics*, 77th ed.; CRC Press: Boca Raton, USA, 1996.
(26) Barthel, J.; Wachter, R.; Gores, H.-J. In *Modern Aspects of Electrochemistry*; Conway, B. E., Bockris, J. O'M., Eds.; Plenum: New York, 1979; Vol. 13.
(27) Barthel, J.; Feuerlein, F.; Neueder, R.; Wachter, R. *J. Solution Chem.* **1980**, *9*, 209.
(28) Stoppa, A.; Hunger, J.; Buchner, R. *J. Chem. Eng. Data* **2009**, *54*, 472.
(29) Hoover, T. B. *J. Phys. Chem.* **1964**, *68*, 876.
(30) Böttcher, C. F. J. *Theory of Electric Polarization*, 2nd ed.; Elsevier: Amsterdam, 1973; Vol. 1.
(31) Böttcher, C. F. J.; Bordewijk, P. *Theory of Electric Polarization*, 2nd ed.; Elsevier: Amsterdam, 1978; Vol. 2.
(32) Hunger, J.; Stoppa, A.; Schrödle, S.; Hefter, G.; Buchner, R. *ChemPhysChem* **2009**, *10*, 723.
(33) Buchner, R.; Chen, T.; Hefter, G. *J. Phys. Chem. B* **2004**, *108*, 2365.
(34) Zasetsky, A. Y.; Buchner, R. *J. Phys.: Condens. Matter* **2011**, *23*, 025903.
(35) Barthel, J.; Buchner, R.; Wurm, B. *J. Mol. Liq.* **2002**, *98*−*99*, 51.
(36) Stewart, J. J. P. *MOPAC2009*, version 9.097W ed.; Stewart Computational Chemistry, 2009.
(37) Barthel, J.; Hetzenauer, H.; Buchner, R. *Ber. Bunsen-Ges. Phys. Chem.* **1992**, *96*, 1424.
(38) Buchner, R.; Hefter, G. T.; May, P. M. *J. Phys. Chem. A* **1999**, *103*, 1.
(39) Hubbard, J.; Onsager, L. *J. Chem. Phys.* **1977**, *67*, 4850.
(40) Hubbard, J. B. *J. Chem. Phys.* **1978**, *68*, 1649.
(41) Szymańska-Cybulska, J.; Kamieńska-Piotrowicz, E. *J. Solution Chem.* **2006**, *35*, 1631.
(42) Kamieńska-Piotrowicz, E.; Stangret, J.; Szymańska-Cybulska, J. *Spectrochim. Acta, Part A* **2007**, *66*, 1.
(43) James, D. W.; Mayes, R. E. *J. Phys. Chem.* **1984**, *88*, 637.
(44) Krumgalz, B. S.; Barthel, J. *Z. Phys. Chem.* **1983**, *142*, 161.
(45) Marcus, Y. *Ion Properties*; Marcel Dekker: New York, 1997.
(46) Ohtaki, H. *Pure Appl. Chem.* **1987**, *59*, 1143.
(47) Sacco, A.; Piccinni, M. C.; Holz, M. *J. Solution Chem.* **1992**, *21*, 109.
(48) Ruben, M.; Walther, D.; Knake, R.; Görls, H.; Beckert, R. *Eur. J. Inorg. Chem.* **2000**, 1055.
(49) Rao, C. P.; Rao, A. M.; Rao, C. N. R. *Inorg. Chem.* **1984**, *23*, 2080.
(50) Asada, M.; Fujimori, T.; Fujii, K.; Kanzaki, R.; Umebayashi, Y.; Ishiguro, S.-i. *J. Raman Spectrosc.* **2007**, *38*, 417.
(51) Eigen, M.; Tamm, K. *Z. Elektrochem.* **1962**, *66*, 107.
(52) Powles, J. G. *J. Chem. Phys.* **1953**, *21*, 633.
(53) Glarum, S. H. *J. Chem. Phys.* **1960**, *33*, 639.
(54) Dote, J. L.; Kivelson, D. *J. Phys. Chem.* **1983**, *87*, 3889.
(55) Alavi, D. S.; Hartman, R. S.; Waldeck, D. H. *J. Chem. Phys.* **1991**, *94*, 4509.
(56) Böttcher, C. F. J. *Recl. Trav. Chim. Pays-Bas* **1946**, *65*, 19.
(57) Fajans, K.; Joos, G. *Z. Phys. A* **1924**, *23*, 1.
(58) Pyper, N. C.; Pike, C. G.; Edwards, P. P. *Mol. Phys.* **1992**, *76*, 353.
(59) Płaczek, A. *Determination of polarizability of the triflate anion in N,N-dimethylformamide by refractive index measurements*. Unpublished results, 2008.
(60) Rittner, E. S. *J. Chem. Phys.* **1951**, *19*, 1030.
(61) Okan, S. E.; Champeney, D. C. *J. Solution Chem.* **1997**, *26*, 405.
(62) For SIPs and 2SIPs such calculations were not possible with MOPAC.
(63) Hunger, J.; Stoppa, A.; Buchner, R.; Hefter, G. *J. Phys. Chem. B* **2009**, *113*, 9527.
(64) Bockris, J. O. M.; Reddy, A. K. N. *Modern Electrochemistry: 1. Ionics*, 2nd ed.; Plenum: New York, 1998.